

Developing Random Network Theory for Carbon Nanotube Modified Electrode Voltammetry: Introduction and Application to Estimating the Potential Drop between MWCNT–MWCNT Contacts

Andrew F. Holloway,[†] David A. Craven,[‡] Lei Xiao,[†] Javier Del Campo,[§] and Gregory G. Wildgoose^{*,†}

Department of Chemistry, Physical and Theoretical Chemistry Laboratory, University of Oxford, South Parks Road, Oxford, OX1 3QZ, United Kingdom, Mathematical Institute, University of Oxford, 24-29 St Giles', Oxford, OX1 3LB, United Kingdom, and Centro Nacional de Microelectrónica, IMB-CNM. CSIC, Campus de la Universidad Autónoma de Barcelona, Bellaterra 08193, Spain

Received: June 1, 2008; Revised Manuscript Received: July 1, 2008

A theoretical model of carbon nanotube (CNT)-modified electrodes is introduced to explain the observed increase in the effective electroactive area of such electrodes when formed by the casting of CNT films on top of an electrode of finite size. The model proposes that a fraction of the CNTs deposited form a conducting network that extends beyond the electrode area and onto the insulating surround. Critical parameters for this situation to occur are described. The random network of conducting CNTs is described by the size of the largest “connected component” and is considered in terms of the minimum number of CNT–CNT connections required to travel a given distance through the network. As such, this approach can be used to describe multilayers of CNTs, provided that the film extends in the radial direction as well as normal to the electrode surface, and also CNTs in contact with more than one neighboring CNT within the mesh. The theoretical predictions were experimentally validated by performing a series of voltammetric experiments. These were conducted using electrodes modified with multiwalled-CNT (MWCNT) films produced by the casting method, so as to deliberately extend the MWCNT film beyond the electrode area. Thus, we determined the magnitude of the potential drop between the first MWCNT–MWCNT contacts to be 20–50 mV. Here we also describe the distribution of potentials throughout the CNT network.

1. Introduction

Since the discovery of multiwalled carbon nanotubes (MWCNTs) in 1976 by Oberlin and Endo^{1,2} (confirmed two years later by Wiles and Abrahamson^{3,4}), their sensational revival in 1991 by Iijima,^{1,5} and the discovery of single-walled carbon nanotubes (SWCNTs) again by Iijima et al. in 1993,^{1,6} closely followed by Behtune et al.,^{1,7} these materials have attracted considerable interest in many different fields of science. The use of carbon nanotubes (CNTs) in electrochemistry was first introduced by Britto and co-workers in 1996.⁸ This area of electrochemistry rapidly expanded after the seminal work of Musameh et al. in 2002.⁹ Since then there are literally thousands of reports that make use of CNT-modified electrodes, for electroanalysis, electrocatalysis, and energy storage applications.^{10,11}

Common methods of immobilizing the CNTs on an electrode surface include: (i) mechanical (abrasive) immobilization, where the electrode is rubbed on a sample of CNTs; (ii) “casting” (also known as the “drop-dry” method), whereby a droplet of a suspension containing CNTs in a volatile solvent is placed on the electrode surface, and the solvent is allowed to evaporate, leaving the CNTs immobilized on the electrode. Voltammetric characterization of the resulting CNT-modified electrodes usually reveals that the electroactive area of the modified electrode has increased in comparison to that of the bare electrode

substrate. This is almost always attributed to the increased microscopic surface area of the electrode imparted by the use of CNTs.^{12,13}

For systems where significant adsorption/deposition of the redox active species of interest on the electrode surface occurs, such as in adsorptive, anodic, or cathodic stripping voltammetry, this explanation is likely correct. However, for the majority of electrochemical experiments where the redox active species of interest is simply diffusing to the electrode surface, that is, where no adsorption on the CNTs occurs and the voltammetric response is purely under “diffusion control” (such as in outer-sphere electron transfer reactions), this explanation can not possibly be correct!

To illustrate this, consider a CNT-modified electrode. The distribution of CNTs on the electrode surface can be considered as a random array of nanobands with the dimensions of the CNTs, for which the relevant theory has been developed elsewhere.^{14–23} If we perform a typical voltammetric experiment, for example the reduction of a 1.0 mM solution of hexaamineruthenium(III) chloride in 0.1 M KCl, then as the electrolysis proceeds, depletion of the redox active species in the region surrounding each CNT in the array will occur, and fresh material will then diffuse down this concentration gradient from bulk solution according to Fick's Laws. Therefore, each CNT in this array will be surrounded by a diffusion layer, the thickness of which (δ) is given by Einstein's equation.¹⁸ Using common experimental parameters, the thickness of the diffusion layer generated around an isolated CNT is ca. 30 μm .¹⁸ Therefore, for each individual CNT on the electrode surface to remain

* Corresponding author. E-mail: gregory.wildgoose@chem.ox.ac.uk; phone: +44 (0)1865 275406; fax: +44 (0)1865 275410.

[†] Physical and Theoretical Chemistry Laboratory, University of Oxford.

[‡] Mathematical Institute, University of Oxford.

[§] Campus de la Universidad Autónoma de Barcelona.

diffusionally independent from its neighbors on the time scale of this experiment, each CNT must be separated by at least 30 μm .

In practice this situation rarely, if ever, occurs. Using any common method of immobilization, the CNTs on the electrode surface are usually in very close proximity to one another (of the order of tens or hundreds of nanometers rather than microns) and, as such, the diffusion layers surrounding each CNT within this random array are heavily overlapping. The situation of heavily overlapping diffusion layers within a random array is classified as type 4 behavior using the Davies–Compton classification,^{14,18,20,21} and results in effectively planar diffusion to the electrode surface. Thus, the maximum electroactive area obtained from a type 4 array would simply be the geometric area covered by that array; in other words, the CNT-modified electrode should produce almost the same electroactive area as that of the bare electrode. Furthermore, Compton and Menshikov have shown that purely diffusion-controlled voltammetry is unaffected by the microscopic surface roughness of an electrode below ca. 50 μm .²⁴

This report provides an explanation for the observed increase in the electroactive area of CNT-modified electrodes, whereby we propose that the tangled mesh of CNTs can extend beyond the area of the underlying electrode surface and onto the insulating surround. As the CNTs are conducting, a proportion of those CNTs on the insulating surround may remain in electrical contact with the electrode, as they are “wired” up by CNT–CNT contacts through the mesh with those CNTs on the electrode surface. Due to the close proximity of tubes in the mesh extending beyond the electrode radius, they form a type 4 random electrode array and, as such, result in an electroactive area covered by the geometric area of the mesh that is larger than that of the bare electrode itself. This hypothesis is based on two observations. First, when using the casting method of immobilizing the CNTs, the volume of the droplet of casting solution used is typically 10–40 μL , and the droplet is typically placed on electrodes 1–3 mm in diameter. As such, the droplet radius is (usually) initially larger than the electrode radius and, therefore, deposits CNTs on the insulating surround beside the electrode surface. Note that abrasive immobilization may also deposit CNTs on the surrounding mantle of the electrode, albeit in a less-controlled manner. Second, the work of Day et al. has shown that a random network of CNTs, which are connected at one end to a gold contact (which is itself subsequently insulated from the electrolyte solution) but which are otherwise supported on an insulating surface, may experience an electrode potential as evidenced by the electrodeposition of metal nanoparticles on the CNTs.²⁵ The size of the nanoparticles decreases with increasing distance from the gold electrode contact, suggesting that there is a distribution of potential through the mesh.

In deriving theory to describe how the random network of CNTs can extend beyond the electrode radius while remaining in electrical contact, we deduce several critical parameters for this condition to be maintained. The latter are easily scaleable to describe any given network of CNTs, with any distribution of lengths and network radius, and are thus widely applicable. The theory is then compared to experiments using standard one-electron redox probes that are positively charged, negatively charged, and neutral in both aqueous and nonaqueous electrolytes. Finally, we demonstrate the first application of this theory to calculate the manner in which the electrode potential varies throughout the random mesh of CNTs, by deliberately casting CNT films onto electrodes that extend beyond the electrode area,

and use this to estimate the voltage drop between MWCNT–MWCNT contacts.

2. Experimental Methods

2.1. Reagents and Equipment. All reagents were purchased from Aldrich (Gillingham, UK), were of the highest commercially available grade, and were used without further purification. Aqueous solutions were prepared using UHQ deionized water from a Millipore (Vivendi, UK) UHQ grade water system with a resistivity of not less than 18.2 $\text{M}\Omega\text{ cm}$ at 298 K. Nonaqueous solutions were dried over 500 \AA molecular sieves and alumina prior to use.

Hollow-tube (h-MWCNTs) and bamboo-like (b-MWCNTs) multiwalled carbon nanotubes (diameter 30 ± 15 nm, length 2–20 μm , purity <95%), and single-walled carbon nanotubes (SWCNTs, purity <95%, length 2–20 μm , diameter 1–2 nm) were purchased from Nanolab (Brighton, MA, USA). The morphology of the b-MWCNTs consists of MWCNTs where the graphene sheets are rolled so as to be at a slight angle to the principal axis of the tube, resulting in many graphene sheets terminating in edge-plane-like sites along the length of the tube. They are also periodically closed off along the tube length into compartments, similar to the structure of bamboo, from which the name derives. In contrast, the h-MWCNTs have the graphene sheets rolled parallel to the principal axis of the tube, and the tubes remain open along their entire length.

Cyclic voltammetry was performed on a $\mu\text{Autolab}$ type III computer-controlled potentiostat (EcoChemie, Utrecht, Netherlands) using a standard three-electrode configuration. A bright platinum wire served as the counter electrode in conjunction with a saturated calomel reference electrode (SCE, Radiometer, Copenhagen, Denmark). The cell assembly was completed using either a gold microelectrode (diameter 120 μm) or a gold macrodisc electrode (BASi Technicol, USA, diameter 1.5 mm) as the working substrate electrode. The electrodes were successively polished using alumina slurry (Beuhler, USA, 3.0–0.1 μm) and sonicated after each polishing to remove any adhered microparticles of alumina. All electrolyte solutions were degassed with pure argon (BOC gases, Guildford, UK) for 30 min prior to commencing any voltammetric measurements.

Where necessary, the electrode was modified with a film of CNTs to form a random CNT network by dropping a 20 μL aliquot of a casting suspension of the desired mass/volume ratio of CNTs to solvent (see below) on the clean electrode and allowing the solvent to evaporate at room temperature.

Scanning electron microscopy (SEM) was performed on a JEOL 6300 instrument with a tungsten filament with an accelerating voltage of 20 kV at an operating distance of 15 mm.

Simulations were performed using the computer algebra package Magma²⁶ on various PCs with 4 GHz processors. Each simulation took approximately 20–30 min, depending on the radius of the domain (A).

3. Results and Discussion

3.1. Building the Model. In this section, we develop a physical model of the mesh of carbon nanotubes (CNTs) and use computational and mathematical techniques to analyze its properties. We begin by describing the model.

Our first assumption is that all the CNTs can be represented as one-dimensional straight lines and that any two CNTs touch each other at a point. The second assumption is that the CNTs are distributed randomly throughout the region covered by the mesh. The final assumption is that there is no resistance along

the tube length and that the only significant contribution to any observable voltage drop occurs at the CNT–CNT contacts. The first assumption will be relaxed somewhat in future work, whereas the second is experimentally confirmed in Section 3.5. Naturally, the third assumption is only an approximation, but the errors involved are likely to be small in relation to the CNT–CNT contacts given that CNTs are reported to have very high electrical conductivity, greater than copper, and the Ohmic drop along a few microns of CNT is, therefore, likely to be negligible for our purposes.

Given these three assumptions, we may develop a model of the CNT mesh as follows: consider a finite region A , which in our case is a circle. We describe a “line in A ” as a straight line connecting two points of A , and not extending beyond those points. Our model of the CNT mesh is then N randomly chosen lines in A , of length given by some distribution, for example, a gamma distribution. We will return to discuss how the distribution of lengths affects the bulk properties of the model later. For example, we may consider 10 000 lines, of mean length 6 μm , lying in a circular region of radius 150 μm . This is then our physical model of the CNT mesh.

From now on, fix a region A and a set L of N lines in A . We are interested in questions such as the following: given two lines α and β in A , is it possible to reach β from α only traveling along lines in L , and if so, how many lines must one use to do so? If α represents a CNT connected to an electrode, then the number of lines transversed should be related to the drop in voltage between the CNT represented by α and that represented by β ; this question, therefore, has physical significance.

Let α and β be two lines in A , and suppose that α is contained in A in such a way that every point of distance at most $|\beta|$ from α is in A . Then the probability that α and β intersect, $P_{\alpha\otimes\beta}$ is (approximately) given by the equation below.

$$P_{\alpha\otimes\beta} = \frac{2|\alpha\beta|}{\pi|A|}$$

Note that the probability would be exactly this value if the line β merely satisfied the condition that only the end-point with the largest y -value need be in A . This calculation is a simple triple integral and is omitted.

If α is a line in A , then the expected number of lines that intersect α is given by the following equation,

$$\frac{2\mu(N-1)|\alpha|}{\pi|A|}$$

where μ is the mean length of the $(N-1)$ other lines in L .

One may also use a computer to derive an estimate for the expected number of lines that cross any given line in the mesh. The computer model will produce a slightly different answer because of the effect of the boundary of A , however this difference is negligible provided that the boundary is at a sufficiently large distance from the center of the mesh, as is the case in the work reported herein.

3.2. The Connected Component and the Effect of the Distribution of CNT Lengths. To better understand the experimental parameters that need to be controlled, we need to understand the “connectedness” of the mesh. To describe this easily, we need to introduce the concept of graphs. A graph (Γ) is a pair (V,E) , where V is a set of vertices, and E is a set of edges, each consisting of two vertices. Two vertices u and v are said to be adjacent if the edge $\{u,v\}$ is in E . Two vertices u and v are said to be connected if there is a sequence of vertices $u = v_0, v_1, \dots, v_n = v$ such that v_i and v_{i+1} are adjacent for all i .

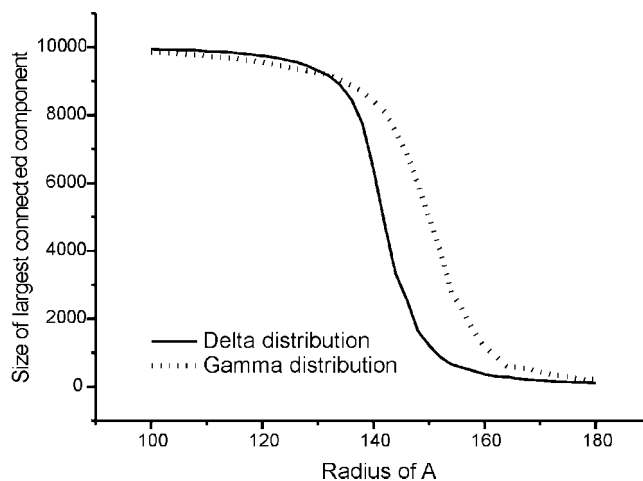


Figure 1. The variation in the size of the connected component against the radius of the area of the mesh for 10 000 randomly distributed lines of mean dimensionless length 6, showing the effect of the δ - and γ -distribution of line lengths.

The physical model we have developed so far may be associated with a graph in the following way: to each line we associate a vertex, and, if two lines are connected to one another, then we include an edge between the two associated vertices. This does not respect the distances of the model, but it does preserve the way in which the lines are connected, which is the important parameter with which we are concerned.

If v is a vertex of Γ , then the “connected component” of Γ containing v is the set of all vertices of Γ connected to v . The set of all connected components of Γ is an important set. It is particularly important for us, because, clearly, for current to be transferred between two CNTs lying on an insulating substrate, the corresponding lines that represent them must be connected.

For us to produce reliable experimental data, we need a very large connected component in our mesh, otherwise we will not be able to transfer current throughout (almost all of) the mesh. Furthermore, we are interested in the relationship between the distance between two points on the mesh, and the (minimum) number of lines connecting the two points. However, to do this we also need to take into account the distribution of lengths of CNTs within the mesh. Therefore, we performed tests using two different models for the lengths of the lines; the first is where they are all of length 6 (a δ -distribution), and the second is where the lines are γ -distributed with mean 6 and variance 6.187 (the reason for this variance is that it correlates with the experimentally measured distribution of lengths obtained using SEM imaging and after scaling, which is described below). Because the δ -distribution can be thought of as a γ -distribution with zero variance, one may, at least qualitatively, get some idea about the situation when lines with different variances are considered by comparing the two sets of data and interpolating or extrapolating as needed.

The size of the connected component and the influence of the different models of CNT length as a function of the radius of the area A for 10 000 lines of dimensionless length 6 are shown in Figure 1. This implies that if the radius is at most, say 100, then we may assume that almost all of the lines form one large connected component. Conversely, if the radius is larger than, say 160, then the CNT mesh on the surface is comprised of many small clumps with connectivity of at most 200. For nanotubes with different size distributions, or other number densities, this graph may be scaled as described below. The important experimental parameter that arises from this is

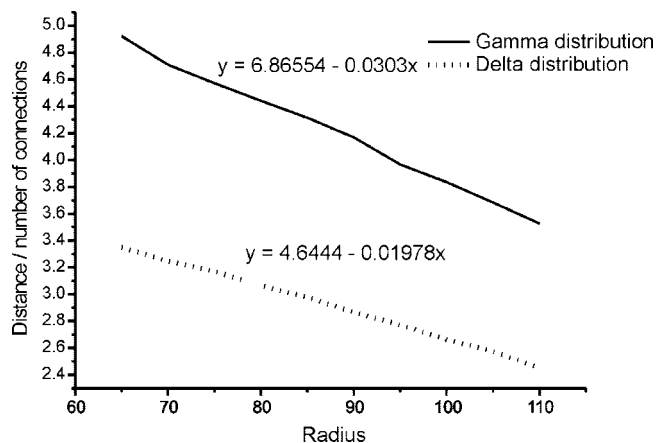


Figure 2. A plot showing the ratio of the distance traversed through the CNT network divided by the number of CNT–CNT connections against the radius of the electroactive area of the mesh. Values derived from the standard model of 10 000 randomly distributed lines of mean dimensionless length 6, showing the effect of the delta and gamma distribution of line lengths.

the critical number density of nanotubes deposited on the electrode surface. For any given size of electrode, it is a simple matter to calculate from Figure 1 (with the appropriate scaling discussed below) the minimum mass of CNTs in any given aliquot of casting solution used, and therefore the required minimum mass/volume ratio of the casting solution. Note that in all the experiments described herein we ensured that we were always working with casting solutions above the critical density to produce networks that consisted (almost) entirely of one single, large connected component, unless stated otherwise.

It seems reasonable that for small radii the gamma-distributed lines should form a smaller connected component than the δ -distributed lines; in the former case, there are small lines that are unlikely to form part of even a large cluster. The opposite would hold for larger radii; in this case, the presence of larger lines in the γ -distributed case can help produce larger components than in the δ -distributed case.

The size of the largest connected component can be easily computed from Figure 1 for any given system of interest using the scaling method described below (the data tables allow the reader to extrapolate the critical number density; therefore, the size of the connected components for any given system of interest may be found in the Supporting Information).

3.3. Scaling and Accounting for Droplet “Roll-up”. The initial experiments that instigated this work were performed using MWCNTs of mean length 6 μm ; thus, the model described above was built to consider this. However, the more detailed experiments described herein were performed on various morphologies of CNTs of mean length 2 μm . This fortuitously provides us with an example of how to scale the model, and the data given in the Supporting Information, to study any given system with differing mean lengths and distribution of lengths of CNTs, thus making the theory developed herein widely applicable. Suppose we have a situation with a number (N) of nanotubes of mean length μ ; we then need to scale this system to the model developed to get the corresponding scaling to the radius. If R denotes the radius of A in the unscaled, real, experimental situation (i.e., N lines of mean length μ , with A corresponding to the droplet size of casting solution used) and r denotes the radius in the scaled situation (i.e., 10 000 lines of mean length 6), then to get the correct scaling we simply use the following expression;

$$\frac{r}{R} = \sqrt{\frac{10,000}{N}} \times \frac{6}{\mu}$$

this is because doubling the radius quadruples the area, and so the number of nanotubes must be quadrupled, and doubling the radius doubles the lengths of lines.

There is a further complication that we must also account for, which is the “roll-up” of the CNTs as the droplet of casting solution evaporates, that is, the tendency for droplets of casting solution to concentrate most of the deposited CNTs into one central clump as the droplet evaporates and the area covered by the droplet shrinks. SEM characterization of CNT networks deposited from a variety of solvents and at different mass/volume ratios is discussed later in Section 3.5. When we image where the CNTs were deposited on a glassy carbon substrate using SEM, it is apparent that the majority of CNTs are deposited in a mesh that can decrease to as little as approximately one-third of the original droplet radius (for example, see the inset in Figure 3a). This is due to the “rolling-up” effect of the CNT suspension as the casting droplet evaporates and therefore decreases in size. As the droplet evaporates some of the CNTs contained in the suspension will be deposited where the droplet is in contact with the substrate surface (usually on the insulating surround, because the droplet is initially much larger than the electrode area), whereas most of the CNTs will still remain in the droplet (which is decreasing in size), until a large cluster of CNTs is deposited. This is shown schematically in Scheme 1. It is difficult to estimate the proportion of CNTs that are deposited on the substrate while the droplet is evaporating and the area it covers shrinks, but from several SEM images (not shown) we estimate that between 20 and 30% of the CNTs are deposited in this way, with the remainder forming the larger clump in the middle. We can demonstrate how to scale the model and account for droplet roll-up by means of the following example, taken from the experimental data discussed below.

The mean length of CNTs used herein is 2 μm , and the number of CNTs deposited in the aliquots of casting solution used is of the order of 2.2×10^7 ; clearly, significant scaling is required. The original droplet radius was estimated to be ca. 3000 μm from the SEM images, but due to droplet roll-up that radius should be decreased to one-third, that is, 1000 μm . In the process of rolling up, we also estimate that the droplet deposits around 20–30% of the CNTs on the surface. We will use both limits, 20 and 30%, of this estimate to gain an insight into the relative magnitude of the error introduced by these approximations. For a 20% loss the number of CNTs remaining in the mesh is now 1.76×10^7 and for a 30% it is 1.54×10^7 , randomly distributed in an area A with an unscaled radius of 1000 μm . Using the scaling formula given above, the corresponding scaled radii for the 20 and 30% case are 71 and 76 respectively. Thus, in this case values of the scaled radius of between 70 and 80 may be reasonable. From Figure 1 it is clear that in both cases we are well-within the region where we have one, large connected component in the CNT mesh, that is, the number density of CNTs deposited in this example is sufficiently above the critical number density.

3.4. Relating the Distance Traveled through the CNT Mesh to the Number of CNT–CNT Connections. Having assured ourselves that we have essentially one connected mesh and how to scale any given experimental situation to the model introduced above, we are now in a position where we could relate the usual (Euclidean) distance in the region A to the distance when one travels on lines only. The mathematical

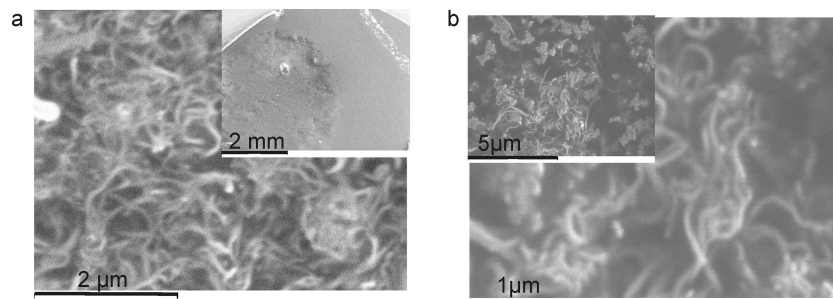
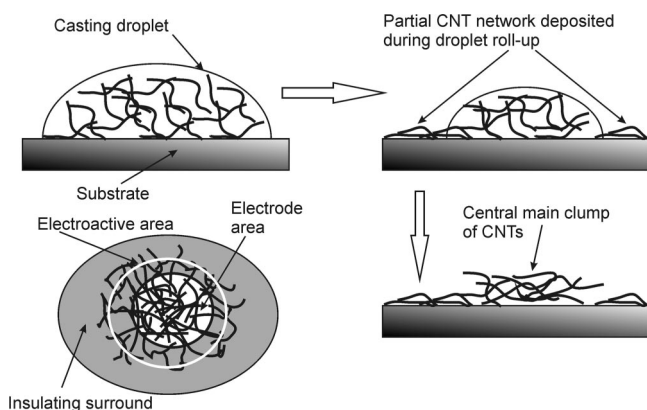


Figure 3. SEM images of the CNT networks deposited from 20 μL aliquots of (a) 1.0 and (b) 0.01 mg per mL suspensions on a glassy carbon stub, showing the connectivity and dispersion of CNTs within the network. Insets: (a) a lower magnification image of the network in panel a, showing the effect of droplet roll-up; (b) a lower magnification image of the network showing the formation of small clumps, rather than one large connected component (note that the small nodular structures are from the underlying substrate and not the CNT network).

SCHEME 1: A diagram showing the effect of droplet “roll-up” on the deposition of CNT films and the resulting extension of the electroactive area (white circle) due to the conducting CNT network



language of metric spaces is one natural treatment of this problem. Let X be a set. A metric on a set X is a function of d such that:

$$d(x, y) \geq 0 \text{ and } d(x, y) = 0 \text{ if and only if } x = y$$

$$d(x, y) = d(y, x)$$

$$d(x, z) \leq d(x, y) + d(y, z)$$

This generalizes the usual concept of distance, with the last axiom being the famous triangle inequality $|x + y| \leq |x| + |y|$. The usual (Euclidean) distance on a region will be denoted by $d_e(x, y)$. Another possible distance function on the mesh is the “mesh distance”, given by the distance $d_m(x, y)$, which is the shortest distance between two points on the mesh traversing only lines in the mesh. If the density of the mesh is infinite, then the two distances, d_e and d_m , are equal. If the density of the mesh is small, then the mesh distance, d_m , should approximate to the square of the Euclidean distance, since the situation is similar to that of a random walk.

We can algebraically relate the mesh distance and the expected number of lines traversed. In practice, it transpires that this method is computationally inefficient. Instead, it is far easier to relate the Euclidean distance and the number of lines traversed directly using the computer model of the mesh, but without moving through the mesh distance, while still maintaining a very high degree of numerical accuracy. This approach will be used throughout.

We are interested in the relationship between the distance between two points on the mesh (d_e) and the minimum number of lines connecting the two points (n_i). Figure 2 shows this information as the ratio of the Euclidean distance (corresponding

to the effective increase in the radius of the electroactive area determined experimentally) and the minimum number (n_i) of CNT–CNT connections (d_e/n_i) for various scaled radii of A , where the lengths of the CNTs are described by either a δ - or a γ -distribution. In the case of the δ -distributed lines, 200 randomly chosen pairs of points were used to compute the mean ratio for each radius. In the case of the γ -distributed lines, 400 randomly chosen pairs of points were used to compute the mean ratio for each radius. More data were needed in the latter case because the variance of the lengths of the lines contributed to an increased variance in the value of this ratio.

It is immediately obvious that there is a linear relationship between the mean ratio (d_e/n_i) and the radius of the region A , in both distributions. The negative correlation is to be expected because, for smaller radii, there will be more paths between two points on the mesh. With more choice of paths, it is likely that shorter paths would exist. The fact that the γ -distributed lines consistently score more highly than the δ -distributed lines is due to lines with larger length allowing larger distances to be covered for each line traversed.

By extrapolation from Figure 2, or by using the tables provided in the Supporting Information, it is now a simple task to calculate the number of CNT–CNT connections traversed for any given distance in the mesh. Simply take the Euclidean distance traversed (i.e., the increase in the radius of the electroactive area) and divide it by the value of the function in Figure 2 corresponding to the radius of the region A . However, it is important to note that the values of the radii on the x -axis are scaled to the model (where 10 000 CNTs of mean length 6 are distributed in a region of 150 μm radius). So, to use these data, one simply has to perform the scaling on the actual experimental parameters used as described above. For example, suppose we experimentally determine that the largest distance traveled through a CNT random network is 35 μm . The value of the corresponding scaled radius in Figure 2 is that given above (71 assuming the case where we have 20% loss due to droplet roll up). At this radius, the mean ratio of distance traveled to the number of CNT–CNT connections is 4.71, assuming a gamma distribution of CNT lengths. Hence, the number of CNT–CNT connections traversed in this example is 7. The values of the mean ratio d_e/n_i for several scaled radii are given explicitly in the Supporting Information to allow the interested reader to extrapolate as necessary.

This model, when used to describe the connectivity of a random CNT network, is particularly powerful, provided thin-layer effects may be neglected (as is the case throughout the work reported herein).²⁷ For example, the model can easily cope with multilayered networks of CNTs (provided that they extend radially beyond the electrode area as well as in the direction

perpendicular to the electrode surface), as any individual CNT that is supported on top of any other CNTs in the mesh, which are themselves connected to the electrode surface through a minimum number of n CNT–CNT connections, is simply considered to be $(n + 1)$ -connected. Similarly, this approach easily deals with CNTs that are connected to more than one other CNT in the mesh. As we are only concerned with the minimum number of CNT–CNT connections required to “wire” any given CNT in the network to the electrode surface, if a given CNT is simultaneously in contact with, say, three other CNTs that are themselves n_i , n_j , and n_k connections from the electrode, and $n_i < n_j < n_k$, then the CNT in question is simply considered to be $(n_i + 1)$ -connected. This latter outcome is particularly useful in our case, because we want to be able to describe the distribution of the applied potential through the CNT mesh as we travel out from the edge of the electrode area to the edge of the CNT mesh on the insulating surround. Because the current will always travel by the path of least resistance, the potential experienced by any given CNT in contact with many other CNTs of differing connectivity (i.e., wired in parallel) will only be determined by the potential on the CNT with the least number of connections back to the electrode.

3.5. Microscopic Characterization of Random CNT Networks. There are many solvents commonly used to cast CNTs onto electrode surfaces.^{28–32} We examined networks of CNTs deposited on a glassy carbon stub from suspensions of MWCNTs in water, acetone, acetonitrile, dimethylformamide, and chloroform, at mass/volume ratios of 0.01, 0.1, and 1.0 mg of MWCNTs per mL solvent, using SEM. Acetone and chloroform were found to produce the best suspensions, as measured by the dispersion within the CNT networks produced; however, the use of acetone was found to produce less than ideal voltammetry, possibly through the formation of a residual layer of solvent on the network; therefore, suspensions in chloroform were chosen throughout this work.

Panels a and b of Figure 3 show the resulting networks deposited from 20 μL aliquots of 1.0 and 0.01 mg per mL suspensions. The former is well-above the critical number density predicted by theory to form one large connected component (which is ca. 1.3×10^6 CNTs/cm² in this case), whereas the latter is below this number. It is apparent that, in the 1.0 mg per mL case, above the critical number density we have a very large connected component. Analysis of the number of connections per nanotube in this image reveals a Poisson distribution of connections centered on three CNT–CNT connections per tube, again in agreement with the theory. In the 0.01 mg/mL case, that is, below the critical density, we see that we do not have one large, connected component: the MWCNTs form numerous small clumps on the substrate. Again, the average number of CNT–CNT connections per tube in these small clumps is distributed around 3, but with a much smaller variance. Therefore, in the 0.01 mg/mL case we would not expect to see any large increase in the effective electroactive area of the MWCNT-modified electrode, as we are unlikely to be able to apply a potential throughout most of the network.

3.6. Voltammetric Characterization of Random CNT Networks. To verify that the predictions of the theory are valid, we performed cyclic voltammetry on CNT-modified gold electrodes with two different diameters, 1.5 mm and 120 μm , using suspensions of CNTs in chloroform that were 0.04 mg/mL (above the critical number density) and 0.01 mg/mL (below the critical number density). We investigated the effect of using CNTs of different morphology, namely the bamboo-like and hollow-tube MWCNTs (b-MWCNTs and h-MWCNTs, respec-

tively) and also using SWCNTs. Furthermore, we investigated the voltammetric response of these CNT networks using 1.0 mM potassium ferrocyanide and 1.0 mM hexaamineruthenium(III) chloride quasi-reversible redox probes in aqueous 0.1 M KCl electrolyte. These redox probes are negatively and positively charged, respectively. We also investigated the response of the CNT-modified electrodes in nonaqueous electrolyte (0.1 M tetrabutylammonium perchlorate, TBAP, in dry dimethylformamide, DMF) using a neutral, reversible redox probe, namely, 1.0 mM ferrocene. In this way we were able to examine the effect(s), if any, of the charge of the redox probe and also the effect of the solvent on the observed voltammetric response; thus, we were able to examine whether the behavior of the network was solely dependent on the properties of the CNTs themselves or whether other factors ought to be considered.

In each case, cyclic voltammetry was performed over the potential region of interest for each redox probe, with the initial potential set so as to be greater than at least 100 mV from the formal potential of each species, and scanned at least 150 mV beyond the peak potential of each species. This ensures that, initially, no Faradaic current is observed due to the redox behavior of each probe and that beyond the peak potential we are in the regime of pure diffusion-controlled voltammetry under a planar diffusive mass transport regime. The voltage scan rate was varied in each case between 10 and 500 mV s⁻¹, and the oxidative and reductive peak currents were recorded. The electroactive area of the CNT-modified electrode and the bare electrode were estimated using the Randles–Ševčík equation.¹⁸

Note that this gives an approximate electroactive area, as the species used are not perfectly reversible. A more accurate approach would be to model the observed voltammetry, for example using the commercial software package Digisim,³³ with the known electrochemical parameters for each species. However, rigorously modeling voltammetry at CNT-modified electrodes is notoriously difficult due to the large background capacitance and sometimes nonideal interactions between CNTs and certain redox probes³⁴ and, possibly, unreliable in light of the variation of voltage through the network. That being said, the Randles–Ševčík approximation will adequately serve our purposes, with only a small error introduced compared to some of the assumptions of the random network theory used.

Panels a–c of Figure 4 show a representative selection of the resulting voltammetric responses for each of the redox probes, solvents, and morphology of CNTs used. In every case shown, where the casting solution used was above the critical number density, a large increase in the peak current is observed, corresponding to a significant increase in the electroactive area. In contrast, when the casting solution used was below the critical number density predicted by the theory, little or no increase in the electroactive area of the CNT-modified electrode is seen compared to that of the bare (unmodified) electrode (data not shown). The average increase (taken from five separate repeat experiments for each case) in the radius of the electroactive area for each system studied is given in Table 1 at both the larger- and smaller-sized gold electrodes modified with a 20 μL aliquot of 0.04 mg/mL CNT suspension in chloroform.

In the case of the two morphologies of MWCNTs at the 1.5 mm diameter electrode, we see an increase in the electroactive area in all cases of around $50 \pm 20 \mu\text{m}^2$, regardless of the redox probe or electrolyte solution used. This could suggest that the factors affecting the CNT–CNT contacts within the network are intrinsic to the MWCNTs themselves, and do not depend on, for example, the nature of the electrolyte, and therefore are not influenced by any

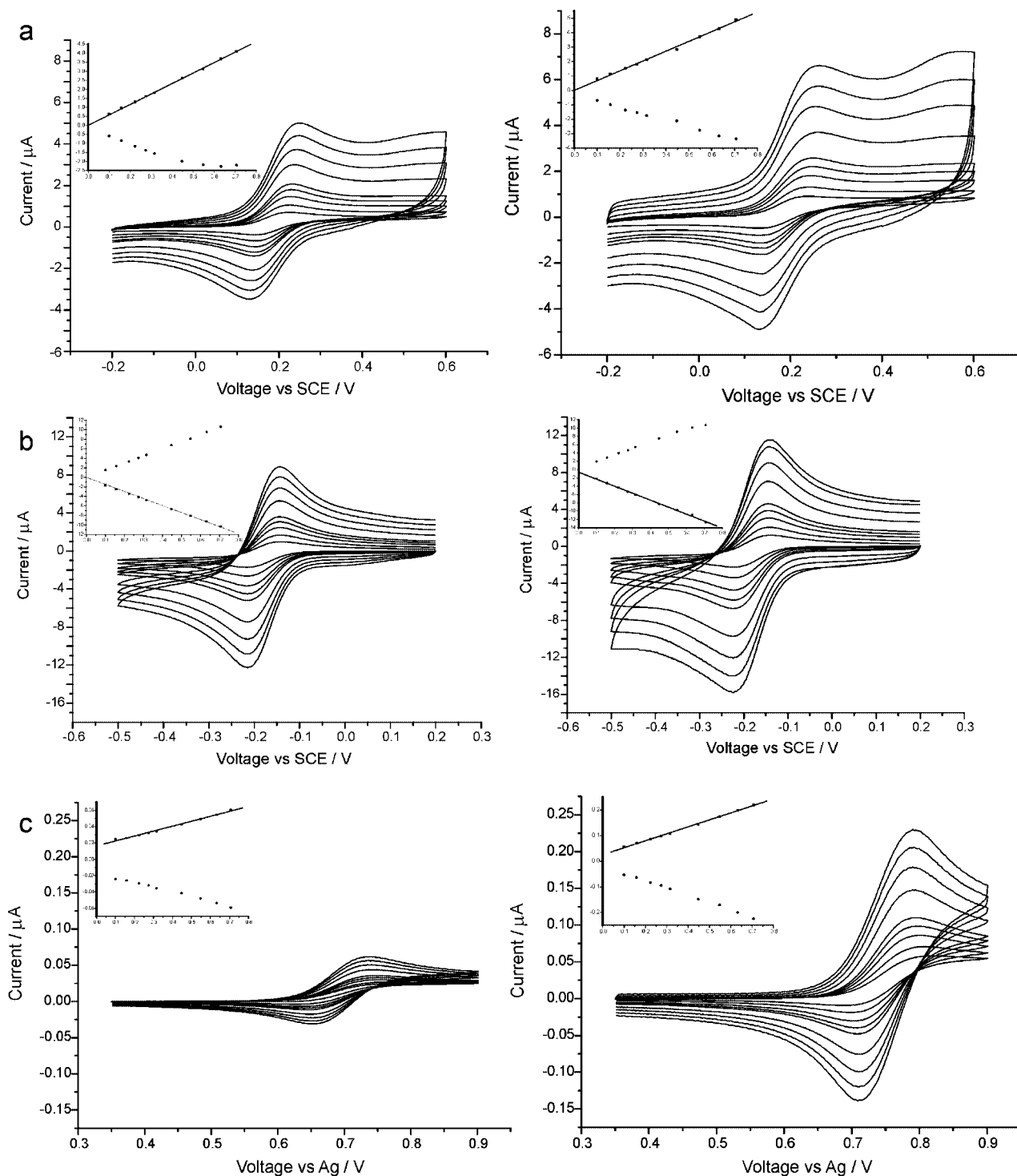


Figure 4. Overlaid cyclic voltammograms recorded at varying scan rates ($10\text{--}500\text{ mVs}^{-1}$) with the corresponding plots of peak current against the square root scan rate inset, comparing: (a) bare 1.5 mm diameter gold electrode (left) and the same electrode modified with h-MWCNTs (right) in 1.0 mM potassium ferrocyanide with 0.1 M KCl; (b) bare 1.5 mm diameter gold electrode (left) and the same modified with b-MWCNTs (right) in 1.0 mM hexamineruthenium(III) chloride with 0.1 M KCl; and (c) bare 120 μm diameter gold electrode (left) and the same modified with b-MWCNTs (right) in 1.0 mM ferrocene with 0.1 M TBAP in DMF.

possible double layer effects that might be envisaged to form between the CNTs if they are separated by a thin layer of electrolyte solution rather than resting in direct contact. We also note that there is no significant difference between the bamboo-like and the hollow-tube MWCNT network's response in this case, suggesting that the manner in which the CNTs are connected as they rest upon and come into contact with each other is the same. In other words, the presence of more conductive edge-plane sites along the

b-MWCNT side walls has little or no observable effect. The degree of variability in the results presented for the MWCNTs on the larger gold electrode probably reflects the slight differences in the CNT networks laid down over each series of experiments and the difficulty in ensuring that the CNT network is deposited with the gold electrode substrate at the center of the mesh. The inconsistency of the results obtained at the smaller 120 μm diameter gold electrode is almost certainly exacerbated by the difficulty in ensuring that the

TABLE 1: The Average Increase^a in the Measured Electroactive Radius of the CNT-modified Gold Electrodes Compared to That of the Bare Electrode^b

modified electrode (diameter)	increase in the radius of electroactive area/ μm		
	1.0 mM $\text{K}_4\text{Fe}(\text{CN})_6 + 0.1 \text{ M KCl}$	1.0 mM $\text{Ru}(\text{NH}_3)_6\text{Cl}_3 + 0.1 \text{ M KCl}$	1.0 mM ferrocene + 0.1 M TBAP in DMF
h-MWCNT ($\phi = 1.5 \text{ mm}$)	40	30	60
h-MWCNT ($\phi = 120 \mu\text{m}$)	36.5	0.7	29
b-MWCNT ($\phi = 1.5 \text{ mm}$)	72	45	52
b-MWCNT ($\phi = 120 \mu\text{m}$)	0.2	1.8	50
SWCNT ($\phi = 1.5 \text{ mm}$)	80	21	16
SWCNT ($\phi = 120 \mu\text{m}$)	10.5	0.2	0.8

^a Taken from five repeat experiments. ^b Recorded for each of the standard redox probes used in aqueous and non-aqueous electrolytes.

CNT network is centrally deposited on the small electrode area. It may also be due to the smaller area of this electrode decreasing the probability of ensuring that enough CNTs within the mesh are initially connected to the electrode surface so as to properly establish a consistently large, single, connected component every time that the electrode is modified. This suggestion is further supported by experiments (not reported here) performed using a gold microelectrode of diameter $20 \mu\text{m}$, where, in our experience, it was rarely possible to ensure good connection of one CNT connected component to the electrode surface. Note that this is consistent with the nature of the CNT network being truly random in that, if this condition is valid one naturally expects there to be gaps and clumps in the network, which may be of sufficient size as to make the network difficult to connect to such a small microelectrode.

In the case of SWCNTs, we note that these results must be treated with caution (i.e., as a qualitative indicator of the SWCNT network behavior), as the dispersion of SWCNTs in solvents such as chloroform is known to be less than perfect, and the SWCNTs are much more likely to be deposited in bundles or “ropes” containing several SWCNTs rather than as individual nanotubes, as is more likely in the case of MWCNTs.³² This then leads to a greater uncertainty in calculating the critical density of required SWCNTs and, indeed, in treating them quantitatively using the theory described herein. The results of the SWCNTs experiments are, therefore, simply presented here for completeness, and the majority of the rest of this discussion refers mainly to the MWCNT-modified electrodes.

The fact that above the critical number density predicted by the theory we generally see a significant increase in the electroactive area and below the critical number density we see no increase in the electroactive area supports our hypothesis that the increase in electroactive area is due to conduction through the CNT network that extends beyond the area of the electrode and onto the insulating surrounding substrate and provides some, tentative, experimental validation of the predictions of the theory.

3.7. Measuring the Voltage Drop Across MWCNT–MWCNT Contacts. Having satisfied ourselves that, for the MWCNT-modified electrodes at least, the random network theory provides a reasonable description of the behavior of CNT-modified electrodes in terms of the observed increase in the electroactive area, we now attempt to apply the theory to estimate the voltage drop between MWCNT–MWCNT contacts. Previous related research in this area, such as measuring the conductivity or resistivity along CNTs, usually involves either complex experimental techniques, such as the use of scanning probe microscopy and the nontrivial litho-

graphic fabrication of single-nanotube junctions between electrodes, or high-level molecular dynamic simulations.^{35–44} Using the random network theory, however, we can estimate the voltage drop between MWCNT–MWCNT contacts simply by modifying a macroelectrode surface with a known amount of MWCNTs and performing cyclic voltammetry in a known solution of any given redox probe. Because the theory is primarily concerned with the minimum number of CNT–CNT connections required to reach any given distance through the mesh, and in doing so can easily account for multiple CNT contacts to any given tube and also multilayers of MWCNTs (provided thin-layer effects are negligible as they are in the work reported herein as evidenced by the voltammetric responses observed), the theory provides an extremely simple yet powerful method of estimating the voltage drop at CNT–CNT contacts. We note that the work of Xu et al.⁴⁰ has already determined that the measured dc conductivity of a SWCNT film network depends on a characteristic distance, which they suggested might be related to the distance between SWCNT–SWCNT contacts, and that this value decreased with increasing density of the film. The theory developed here, where we describe a network in terms of the number of connections, complements its findings and might provide some verification of its hypothesis.

The resistance between each CNT–CNT contact in the network should not vary with the distance from the electrode, as the contacts are of the same nature throughout. As such, the potential drop experienced at each contact should be a constant proportion of the initial voltage. Otherwise, applying an infinite voltage would result in zero potential drop, and the size of the electroactive area would depend on the redox potential of the electroactive species, rather than on the properties of the network (i.e., its connectivity) itself. Therefore, the potential through the CNT network should decay exponentially from the initial value of the electrode itself (V_i), which physically corresponds to the peak potential in the cyclic voltammogram, to some value at a distance through the network corresponding to the increase in the electroactive radius (V_f). Physically, V_f corresponds to the onset potential in the cyclic voltammogram where the Faradaic current begins to flow. The potential at any intermediate point throughout the network (V_n) is simply related to the number of CNT–CNT connections (n) that point away from the electrode substrate by the following equation.

$$V_n = ab^n$$

The constants a and b can simply be evaluated from the boundary conditions that, at $n = 0$, then $V_n = V_i$, and that at

TABLE 2: The Percentage Drop Per CNT–CNT Contact and the Absolute Magnitude of the Potential Drop Across the First CNT–CNT Connection from the Electrode Surface (at $n = 1$)^a

type of MWCNT	% voltage drop per CNT–CNT contact			absolute potential drop at $n = 1$ /mV		
	1.0 mM $K_4Fe(CN)_6$ + 0.1 M KCl	1.0 mM $Ru(NH_3)_6Cl_3$ + 0.1 M KCl	1.0 mM ferrocene + 0.1 M TBAP in DMF	1.0 mM $K_4Fe(CN)_6$ + 0.1 M KCl	1.0 mM $Ru(NH_3)_6Cl_3$ + 0.1 M KCl	1.0 mM ferrocene + 0.1 M TBAP in DMF
h-MWCNTs	15.2% (12.7%)	24.5% (17.1%)	2.4% (1.7%)	37.4 (31.2)	52.6 (36.6)	19.0 (13.4)
b-MWCNTs	8.4% (5.8%)	14.7% (10.7%)	2.7% (1.9%)	19.0 (13.1)	31.5 (22.9)	22.0 (15.4)

^a Determined using each redox probe assuming a γ -distribution of CNT lengths. Numbers in brackets correspond to a δ -distribution of lengths.

the limit of the electroactive area, which is n_f connections from the electrode, then $V_n = V_f$, so that the expression for the potential at any point in the electroactive connected component of the CNT mesh is simply:

$$V_n = V_i \left(\sqrt[n_f]{\frac{V_f}{V_i}} \right)^n$$

Given that the initial and final potentials are known from the cyclic voltammogram, as is the radius of the electroactive area, all that remains is to relate this radius to the corresponding number of connections (n_f) using the appropriately scaled values in Figure 2 (and the Supporting Information). Doing this gives the results presented in Table 2 for the b-MWCNTs and the h-MWCNTs, assuming both a γ - and δ -distribution of lengths.

Note that because we are considering the percentage voltage drop per MWCNT–MWCNT contact, the values in the case of ferrocene are smaller than those obtained in the aqueous electrolytes due to the larger absolute values of the potentials in the former case. However, if we consider the absolute magnitude of the potential drop across the first MWCNT–MWCNT contact from the electrode surface (i.e., at $n = 1$), we see that the values are of a similar magnitude in all cases, being of the order of 20–50 mV. Note that the absolute magnitude of the potential drop then decreases as the number of connections away from the electrode increases. It is interesting to note that the potential drop at the b-MWCNT connections is typically less than that at the h-MWCNTs. Without wishing to over-interpret the data, we tentatively propose that this may reflect the increased number of electroactive (and therefore more conducting) edge-plane defect sites along the length of the b-MWCNTs compared to the h-MWCNTs.

4. Conclusions

Theory has been introduced and developed that explains the observed increase in the electroactive area of electrodes modified with films of CNTs in terms of a random conducting network of CNTs, which is thereby capable of extending beyond the area of the underlying electrode substrate onto the insulating surrounding substrate. The theory is used to calculate the minimum number of connections between CNTs required to travel a given distance within this random network. As such, it is capable of dealing with the realistic situation of multilayer formation (provided that thin layer effects can be neglected) and also to CNTs connected to more than one other CNT in the network. It also introduces the concept of a critical number density of CNTs required to form one large connected component. Above this critical number density an increase in the electroactive area is experimentally indeed observed, whereas below this value the measured electroactive area is simply that

of the bare electrode substrate, thus verifying the predictions of the model. Concepts of scaling are introduced to ensure that the results of the model presented are applicable to any experimental situation, and are therefore of value to the reader (see Supporting Information for relevant data). A qualitative treatment of the effect of droplet “roll-up” is given, although a more rigorous treatment of this effect will be the subject of future work. The effect of the different possible distribution of CNT lengths is also described.

The theory has been applied to a simple experiment where, by simply performing voltammetry at an electrode modified with a known quantity of CNTs (above the critical number density), which was deliberately formed so as to extend the CNT film beyond the electrode area, and using a solution of a standard redox probe, one can estimate the magnitude of the potential drop between CNT–CNT contacts. This latter result may be pertinent to wider research areas involving films or composites of CNTs, such as the use of CNTs in electronic circuit design, CNT-based electrochemical sensors, electrodeposition of metal nanoparticles onto CNT films, scanning probe microscopic techniques such as scanning tunneling microscopy and electrochemical variants on this method that use CNTs as nanometer-sized probe tips, and energy storage devices such as super capacitors. It is also of direct relevance to electrochemical impedance spectroscopic (EIS) studies of CNT-modified electrodes, as the information that can be obtained from EIS studies is strongly dependent on the chosen model of the system being studied and the assumptions inherent therein used to construct equivalent circuits.

Future work will seek to improve the theory by considering the curvature of CNTs within the network, which should result in a decrease in the estimated value of the voltage drop, and also to investigate the effect the distribution of potential within the CNT network has on the electron transfer kinetics and the resulting voltammetric response of such an electrode.

Acknowledgment. G.G.W. thanks St John’s College, Oxford, for a Junior Research Fellowship. D.A.C. thanks Christ Church College, Oxford, for a Junior Research Fellowship. J.D.C. thanks the Spanish Ministry of Education for a Ramón y Cajal Fellowship.

Supporting Information Available: Excel spreadsheets relating to the size of the connected component against the radius of the CNT network and to the ratio of the minimum number of connections per distance against the radius of the CNT network may be found in the Supporting Information. This material is available free of charge via the Internet at <http://pubs.acs.org>.

References and Notes

- (1) Monthieux, M.; Kuznetsov, V. L. *Carbon* **2006**, *44*, 1621.
- (2) Oberlin, A.; Endo, M. *J. Cryst. Growth* **1976**, *32*, 335.
- (3) Abrahamson, J.; Wiles, P. G.; Rhoades, B. L. *Carbon* **1999**, *37*, 1873.
- (4) Wiles, P. G.; Abrahamson, J. *Carbon* **1978**, *16*, 341.
- (5) Iijima, S. *Nature* **1991**, *354*, 56.
- (6) Iijima, S.; Ichihashi, T. *Nature* **1993**, *363*, 603.
- (7) Bethune, D. S.; Kiang, C. H.; de Vries, M. S.; Gorman, G.; Savoy, R.; Vazquez, J.; Beyers, R. *Nature* **1993**, *363*, 605.
- (8) Britto, P. J.; Santhanam, K. S. V.; Ajayan, P. M. *Biochem. Bioenerg.* **1996**, *41*, 121.
- (9) Musameh, M.; Wang, J.; Merkoci, A.; Lin, Y. *Electrochem. Commun.* **2002**, *4*, 743.
- (10) Wildgoose, G. G.; Banks, C. E.; Compton, R. G. *Small* **2006**, *2*, 182.
- (11) Wildgoose, G. G.; Banks, C. E.; Leventis, H. C.; Compton, R. G. *Microchim. Acta* **2006**, *152*, 187.
- (12) Gouveia-Caridade, C.; Pauliukaite, R.; Brett, C. M. A. *Electrochim. Acta* **2008**.
- (13) Liu, A.; Honma, I.; Zhou, H. *Biosens. Bioelectron.* **2007**, *23*, 74.
- (14) Davies, T. J.; Moore, R. R.; Banks, C. E.; Compton, R. G. *J. Electroanal. Chem.* **2004**, *574*, 123.
- (15) Banks, C. E.; Davies, T. J.; Wildgoose, G. G.; Compton, R. G. *Chem. Commun.* **2005**, 829.
- (16) Streeter, I.; Xiao, L.; Wildgoose, G. G.; Compton, R. G. *J. Phys. Chem. C* **2008**, *112*, 1933.
- (17) Streeter, I.; Fietkau, N.; Del Campo, J.; Mas, R.; Munoz, F. X.; Compton, R. G. *J. Phys. Chem. C* **2007**, *111*, 12058.
- (18) Compton, R. G.; Banks, C. E. *Understanding Voltammetry*; World Scientific: Singapore, 2007.
- (19) Ordeig, O.; Banks, C. E.; Davies, T. J.; del Campo, J.; Munoz, F. X.; Compton, R. G. *J. Electroanal. Chem.* **2006**, *592*, 126.
- (20) Davies, T. J.; Banks, C. E.; Compton, R. G. *J. Solid State Electrochem.* **2005**, *9*, 797.
- (21) Davies, T. J.; Compton, R. G. *J. Electroanal. Chem.* **2005**, *585*, 63.
- (22) Davies, T. J.; Ward-Jones, S.; Banks, C. E.; Del Campo, J.; Mas, R.; Munoz, F. X.; Compton, R. G. *J. Electroanal. Chem.* **2005**, *585*, 51.
- (23) Streeter, I.; Compton, R. G. *J. Phys. Chem. C* **2007**, *111*, 15053.
- (24) Menshikov, D.; Streeter, I.; Compton, R. G. *J. Phys. Chem. C* in press, **2008**.
- (25) Day, T. M.; Unwin, P. R.; Wilson, N. R.; Macpherson, J. V. *J. Am. Chem. Soc.* **2005**, *127*, 10639.
- (26) Bosma, W.; Cannon, J.; Playoust, C. *J. Symbolic Comput.* **1997**, *24*, 235.
- (27) Streeter, I.; Wildgoose, G. G.; Shao, L.; Compton, R. G. *Sensors Act. B* **2008**, *B133*, 462–466.
- (28) Hwang, J.-Y.; Nish, A.; Doig, J.; Douven, S.; Chen, C.-W.; Chen, L.-C.; Nicholas, R. J. *J. Am. Chem. Soc.* **2008**, *130*, 3543.
- (29) Lee, J.; Kim, M.; Hong, C. K.; Shim, S. E. *Meas. Sci. Technol.* **2007**, *18*, 3707.
- (30) Lee, J.-H.; Paik, U.; Choi, J.-Y.; Kim, K. K.; Yoon, S.-M.; Lee, J.; Kim, B.-K.; Kim, J. M.; Park, M. H.; Yang, C. W.; An, K. H.; Lee, Y. H. *J. Phys. Chem. C* **2007**, *111*, 2477.
- (31) Dumonteil, S.; Demortier, A.; Dettriche, S.; Raes, C.; Fonseca, A.; Ruhle, M.; Nagy, J. B. *J. Nanosci. Nanotechnol.* **2006**, *6*, 1315.
- (32) Fu, K.; Sun, Y.-p. *J. Nanosci. Nanotechnol.* **2003**, *3*, 351.
- (33) BASi, Digisim Simulation Software for Cyclic Voltammetry, www.bioanalytical.com/products/ec/digisim/.
- (34) Holloway, A. F.; Wildgoose, G. G.; Compton, R. G.; Shao, L.; Green, M. L. H. *J. Solid State Electrochem.* **2008**, DOI 10.1007/s10008.
- (35) Tchoul, M. N.; Ford, W. T.; Ha, M. L. P.; Chavez-Sumarriva, I.; Grady, B. P.; Lolli, G.; Resasco, D. E.; Arepalli, S. *Chem. Mater.* **2008**, *20*, 3120.
- (36) Wang, D.; Song, P.; Liu, C.; Wu, W.; Fan, S. *Nanotechnol.* **2008**, *19*, 075609/1.
- (37) Nagapriya, K. S.; Berber, S.; Cohen-Karni, T.; Segev, L.; Srur-Lavi, O.; Tomanek, D.; Joselevich, E. *Condensed Matter* **2008**, *1*.
- (38) Conwell, E. M. *Nano Lett.* **2008**, *8*, 1253.
- (39) Kauffman, D. R.; Star, A. *J. Phys. Chem. C* **2008**, *112*, 4430.
- (40) Xu, H.; Zhang, S.; Anlage, S. M.; Hu, L.; Gruner, G. *Condensed Matter* **2007**, *1*.
- (41) Vanmaekelbergh, D.; Houtepen, A. J.; Kelly, J. J. *Electrochim. Acta* **2007**, *53*, 1140.
- (42) Osman, M. A.; Cummings, A. W.; Srivastava, D. *Topics Appl. Phys.* **2007**, *109*, 154.
- (43) Liang, W.; Bockrath, M.; Park, H. *Annu. Rev. Phys. Chem.* **2005**, *56*, 475.
- (44) McGuire, K.; Rao, A. M. *Carbon Nanotubes* **2005**, 117.